Arabian Journal of Chemistry (2019) 12, 1447–1453

King Saud University

Arabian Journal of Chemistry

www.ksu.edu.sa
www.sciencedirect.com

ORIGINAL ARTICLE

Red shifting of absorption maxima of phenothiazine based dyes by incorporating electron-deficient thiadiazole derivatives as π-spacer

Asif Mahmood [a,*], Salah Ud-Din Khan [b], Usman Ali Rana [b], Mudassir Hussain Tahir [a]

[a] *Department of Chemistry, University of Sargodha, Sargodha 40100, Pakistan*
[b] *Sustainable Energy Technologies Center, College of Engineering, King Saud University, P.O. Box 800, Riyadh 11421, Kingdom of Saudi Arabia*

Received 15 August 2014; accepted 3 November 2014
Available online 7 November 2014

KEYWORDS

Organic dyes;
Dye sensitized solar cells;
Phenothiazine dyes;
Density functional theory

Abstract This study was carried out to design phenothiazine based dyes by incorporating electron-deficient thiadiazole derivatives as π-spacer. Density functional theory and time-dependent density functional theory calculations of the geometries, electronic structures and absorption spectra of the dyes before and after binding to titanium oxide were carried out. Effects of the electron-deficient units on the spectra and electrochemical properties have been investigated. Compared with the reference compound CS1A, Dyes 1–4 display remarkably enhanced spectral responses in the red portion of the solar spectrum. The newly designed dyes demonstrate desirable energetic and spectroscopic parameters, and may lead to efficient metal-free organic dye sensitizers for DSSCs.

1. Introduction

In the past two decades, dye-sensitized solar cells (DSSCs) have attracted significant attention from the research community because they emerged as the potential alternatives for the next-generation photovoltaic devices (O'Regan and Grätzel, 1991). The sensitizer is one of the key components in DSSCs and plays a critical role in power conversion efficiency as well as device stability (Abdullah et al., 2013). A wide range of photosensitizers, including metal complexes, porphyrins, phthalocyanines and metal-free organic dyes, have been designed and applied to DSSCs (Boschloo and Hagfeldt, 2009). Among the several known dye sensitizers, ruthenium complexes showed overall conversion efficiency over 11% (Nazeeruddin et al., 2005). However, besides being the most efficient material among the other known sensitizers, the large scale use of ruthenium based dye sensitizers is limited due to their significantly high cost, scarce natural reserves of ruthenium and environmental concerns (Abdullah et al., 2013). In order to address these aforementioned challenges associated with metal based dye sensitized cells, metal-free organic sensitizers are therefore seen as emerging class of materials that

* Corresponding author.
E-mail address: asifmahmood023@gmail.com (A. Mahmood).
Peer review under responsibility of King Saud University.

Production and hosting by Elsevier

http://dx.doi.org/10.1016/j.arabjc.2014.11.007

display several potential advantages in DSSC applications (Mishra et al., 2009; Choi et al., 2010). Some features of these metal-free organic dye sensitizers include affordable cost, appreciable durability, and inherent environmentally benign nature along with absorption and electrochemical properties (Irfan et al., 2013).

Laboratory development of D-π-A dyes often invokes a trial-and-error approach, which requires extensive chemical synthesis and expensive materials processing with a slow progress. In this regard, theoretical screening of potential organic dyes using state-of-the-art first principles computation shows great promise, significantly reducing the cost to develop efficient dyes and expediting discovery of new ones.

Phenothiazines (PTZ) are well-known heterocyclic compounds with electron-rich sulfur–oxygen and nitrogen heteroatoms. Organic sensitizers containing phenothiazine have recently attracted considerable research interests on account of their unique excellent hole-transporting ability, rigid structure and large π-conjugated system (Qiu et al., 2008).

Phenothiazine is selected as electron donor due to following reasons: (1) it contains electron-releasing nitrogen and sulfur heteroatoms; (2) it is nonplanar, and therefore can decrease molecular aggregation (Wu et al., 2010). Moreover, the alkyl group suppresses dye aggregation and dark current. Phenothiazine (PTZ) based dye, CS1A which was previously studied by Agrawal et al. (2013) was selected as reference compound to design new dyes.

To obtain a higher light to energy conversion efficiency a sensitizer with high molar extinction coefficients and absorbance in whole visible/near-IR regions is required. It is demonstrated that a sensitizer with longer π-conjugations shows higher molar extinction coefficients and light harvesting efficiency, thus leading to higher DSSC efficiency and stability (Zeng et al., 2010). As compared with metal based sensitizers, organic sensitizers show sharp and narrow absorption bands in the visible region, which impairs light-harvesting capabilities.

Electron-withdrawing terephthalonitrile (Tian et al., 2008) or electron-deficient heteroarenes including pyrimidine (Lin et al., 2011) and benzothiadiazole (Lee et al., 2011; Thomas et al., 2011; Velusamy et al., 2005) unites have been incorporated to dyes as π spacer to lower LUMO energy levels. The newly designed dyes showed more red-shifted absorption bands and high light harvesting than their electron-rich analogs, such as thiophene derivatives (Xu et al., 2008), furan (Lin et al., 2009), and pyrrole (Yen et al., 2008). Lee et al. (2011) have reported the synthesis of TPA organic dyes having benzothiadiazole and the new dyes showed red-shift in the absorption spectra due to the longer π-conjugation and narrow HOMO–LUMO gap (Agrawal et al., 2013). Thomas et al., 2011 demonstrated that the introduction of the electron-deficient dithienylbenzothiadiazole group to the anthracene-based TPA dye resulted in a 50 nm red-shifted band and an increase in intensity.

In this study, organic D-π-A dyes are designed using PTZ donors and cyanoacrylic acid acceptors, bridged by various electron-deficient thiadiazole derivatives. The electron-deficient units considered here involve 2,1,3-benzothiadiazole (BT) and thiadiazolo[3,4-c]pyridine (PyT), which have been shown to lower LUMO levels of the organic molecules while at the same time maintain HOMO levels, thus leading to a smaller HOMO–LUMO gap, and a more red-shifted UV/Vis spectrum (Lee et al., 2011; Thomas et al., 2011; Velusamy et al., 2005). To further lower the HOMO–LUMO gap, a naphtho[2,1-b:3,4-b′]dithiophene (NDT) unit is connected to BT or PyT to lift the HOMO energy levels. The structures of the dyes studied in this work are shown in Fig. 1. The new PTZ dyes are denoted as Dyes 1–4. A model dye CS1A with no π-spacer was also studied for parallel comparison. Calculations were done using density functional theory (DFT), and time-dependent DFT (TDDFT) approaches to demonstrate the effects of the electron-deficient units on the spectra and electrochemical properties of the PTZ organic dyes.

2. Computational details

All the calculations were performed with the Gaussian 09 program package (Frisch et al., 2009). Structure optimization of the ground state of the dyes before and after binding to the $Ti_5O_20H_{22}$ cluster in gas phase has been performed by using B3LYP functional and 6–31 + G* basis set for non-metal atoms while LANL2DZ basis set for the Ti atom. Absorption spectrum of CS1A was computed using different functionals to check the accuracy of functionals. Experimental and theoretical λ_{max} calculated using different functionals are presented in Table 1. Experimental value of λ_{max} of CS1A is 438 nm in THF (Agrawal et al. (2013). From Table 1 it is clear that λ_{max} is functional dependent because it is significantly changed

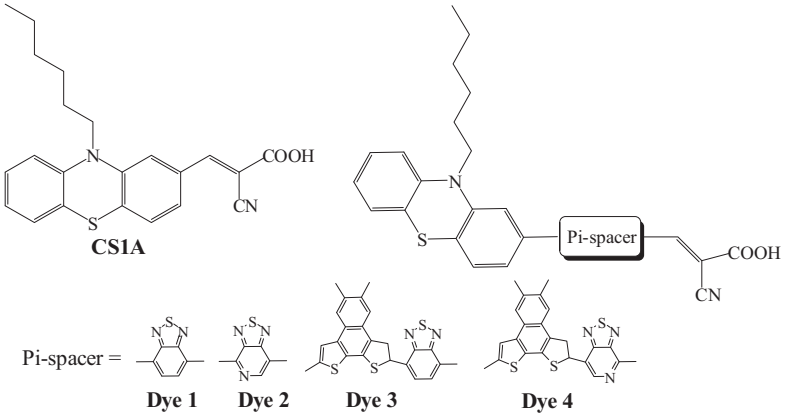

Figure 1 Structures of studied dyes.

Table 1 TD-DFT data of CS1A dye calculated using different functionals.

Functional	λ_{max}	f	Main configuration
B3LYP	532	1.420	H → L (70%)
PBE0	475	1.745	H → L (98%)
BH and HLYP	462	1.342	H → L (94%)
CAM-B3LYP	456	0.902	H → L (90%)
LC-BLYP	450	0.673	H → L (87%)
Experimental	438*		

* Experimental values in THF (Agrawal et al., 2013).

with the change of functional. Values of λ_{max} calculated using B3LYP was higher than experimental λ_{max} by 94 nm. PBE0, BH and HLYP as compared with B3LYP gave a relatively good performance in the prediction of λ_{max}. In this study CAM-B3LYP showed results almost similar to experimental (with error of 14 nm). Among all functionals, LC-B3LYP showed the minimum error in the estimation of λ_{max} (12 nm). Therefore, on the basis of the agreement with experimental data, LC-BLYP is selected to simulate the UV/Vis spectra of designed dyes. LC-BLYP provides a consistent picture of charge-transfer excitations as a function of molecular size (Wong and Cordaro, 2008). The 6–31 + G* for C, H, O, N, S atoms and LANL2DZ for Ti atom have been selected for the calculation of absorption spectra. The absorption spectra of the dyes before and after binding to the $Ti_5O_{20}H_{22}$ cluster were simulated by TD-DFT. Solvent effect (THF) was undertaken using conductor-like polarizable continuum model (CPCM) (Barone and Cossi, 1998).

3. Results and discussion

In this study, we presented the results of theoretical designing of efficient sensitizers for dye sensitized solar cells. Structures of dyes are shown in Fig. 1.

3.1. Energy level alignment

The energy level of HOMOs and LUMOs of the dye sensitizer should match with iodine/iodide redox potential and the conduction band edge level of the TiO_2 semiconductor (Qin et al., 2007). The energy level diagram of the HOMO and LUMO of the dyes, E_{cb} of TiO_2 and redox potential energy of the electrolyte are presented in Fig. 2. For all dyes considered here, the simulated LUMOs lie above the TiO_2 conduction band edge (4.00 eV in vacuum) (Gratzel, 2001), providing the thermodynamic driving force for favorable electron injection from the excited state dye to the TiO_2 conduction band edge. Meanwhile the HOMOs of all dyes lie below the iodide redox potential (4.80 eV in vacuum) (Zhang et al., 2009), leading to a fast dye regeneration and avoiding the geminate charge recombination between oxidized dye molecules and photo-injected electrons in the nanocrystalline TiO_2 film.

From Fig. 2, we can observe a significant change in the energy of molecular orbitals of PTZ dyes on the modification of π-bridge unit. The addition of highly electron-deficient BT unit in Dye 1 effectively lowered the LUMO of Dye 1 to −3.11 eV compared with that of CS1A (−2.50 eV). Due to the significant decrease of the LUMO level, the HOMO–LUMO gap of Dye 1 is 2.50 eV smaller than that of CS1A. Similar features for CS1A and Dye 2 are also found. Pyridine is electron deficient as compared with benzene. Therefore in the BT unit benzene is replaced with a pyridine group, the resulting unit, thiadiazolo[3,4-c]pyridine (PyT), is expected to be a stronger electron-deficient group. In Dyes 2 and 4, we have replaced the electron-deficient BT unit with the more electron-deficient PyT units. This strategy significantly lowered the LUMO energy and therefore decreased the HOMO–LUMO energy gap.

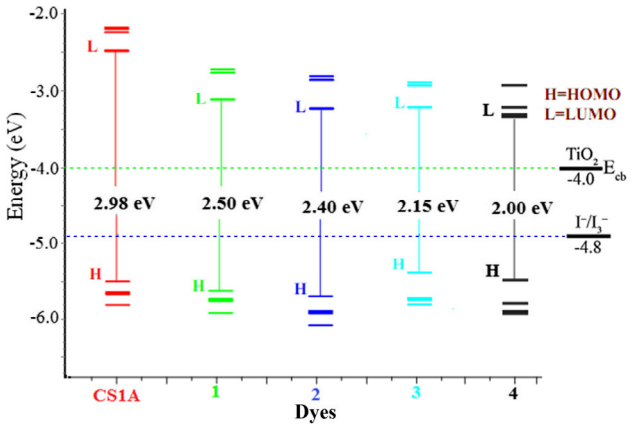

Figure 2 Schematic energy diagram of dyes, TiO_2 and electrolyte (I^-/I_3^-), E_{HOMO} and E_{LUMO} of the dyes.

3.2. NBO electron distribution analysis

We estimated the charge distributions of dye-TiO_2 at both the ground state and the first excited state to qualitatively determine the number of photoinduced electrons from the excited state of the dye to TiO_2 cluster by natural bond orbital (NBO) analysis. Based on the D-π-A architecture, the positive charges of the donor group and π-conjugated linker of all dyes demonstrated them as being an effective electron-pushing unit. In contrast, the negative charges in the anchoring group, shows that they are an effective electron-pulling unit which traps the electron in the molecular backbone. During photoexcitation, the electrons could be successively transferred through the p-conjugated spacer from the donor group to the acceptor, and finally injected into the semiconductor TiO_2 conduction band. As seen in Table 2, charge differences of TiO_2 between S_1 and S_0 in all sensitizers indicate that the electron transmission in Dyes 1–4 is prominent than CS1A dye.

3.3. UV–Vis spectra of dyes

To gain insights into the excited states giving rise to the intense absorption spectra of sensitizers, TD-DFT calculations were performed at the LC-BLYP/6–31 + G* level using C-PCM in THF. In the TD-DFT calculations of absorption spectra, the 10 lowest singlet–singlet transitions were taken into account.

Computed maximum absorption wavelengths (λ_{max}), absorption energy, oscillator strengths (f) and nature of the transitions are listed in Table 3. All dyes showed absorption

Table 2 Natural bond orbital analysis (atomic charge) of the ground state (S_0) and excited state (S_1) of dyes.

Dye	S_0				S_1				Δq[a]
	D	π	A	TiO_2	D	π	A	TiO_2	
CS1A	0.174	0.094	−0.161	0.314	0.244	0.129	−0.221	0.309	0.005
1	0.199	0.099	−0.243	0.326	0.264	0.128	−0.288	0.303	0.023
2	0.274	0.104	−0.279	0.342	0.344	0.139	−0.339	0.324	0.018
3	0.291	0.121	−0.316	0.356	0.356	0.15	−0.361	0.337	0.019
4	0.332	0.132	−0.638	0.367	0.402	0.167	−0.698	0.343	0.024

[b]Unit in a.u.
[a] Δq is the charge differences on TiO_2 between S_1 and S_0.

Table 3 Computed maximum absorption wavelengths (λ_{max}/nm), absorption energy (E_g/eV), oscillator strengths (f), light harvesting efficiency (LHE) and transition natures of dyes.

Dye	λ_{max}	E_g	f	LHE	Main configurations
CS1A	450	2.98	0.673	0.706	H → L (87%)
1	501	2.50	0.864	0.863	H → L (87%)
2	536	2.40	0.973	0.894	H → L (65%)
3	562	2.15	1.161	0.931	H-1 → L (74%)
4	577	2.00	1.223	0.940	H → L (63%)

in the visible region (450–577 nm). Absorbance in the visible region is required for high efficiency. Oscillator strengths were also high (0.673–1.223).

Compared with dye CS1A the introduction of BT, PyT, NDT-BT, and NDT-PyT moieties reveals strong effects on the UV/Vis spectra and leads to remarkably red-shifted adsorption bands. In the case of Dye 1, the incorporation of a BT unit displays a remarkable 51 nm red-shifting absorption than CS1A. The BT unit is a low-band gap chromophore which can significantly affect the electronic structure of the dye and reduces the band gap tremendously by lowering the LUMO energy level and therefore resulting to a red-shifted adsorption (Thomas et al., 2011). PyT is expected to be a stronger electron-deficient unit than BT. Table 3 demonstrates that Dye 2 showed a more red-shifted absorption of 86 nm than CS1A, which might enhance the light harvesting of the sensitizers. For Dyes 1 and 2 with similar structural architecture, Dye 2 displays a 35 nm red-shifted absorption band when compared to Dye 1, due to the fact that the pyridine unit is a much stronger π-electron deficient unit.

Dyes 3 and 4 are constructed with the presence of the NDT group to the π spacer. Table 3 clearly shows that the incorporation of NDT and electron-deficient thiadiazole derivatives into the π-spacer shifted the absorption band to the red portion of the solar spectrum. Organic Dye 3 exhibited absorbance maxima at 562 nm, which red-shifted 112 nm relative to CS1A dye, while Dye 4, on introducing NDT and the more electron-deficient PyT unit, showed a significant red-shift of 127 nm as compared with CS1A dye. Efficiency of DSSC also depends on the Light harvesting efficiency (LHE) that can be enhanced by increasing molar extinction coefficient and extending the spectral absorption range. Photocurrent can also be increased by increasing LHE. Theoretically, the LHE is calculated using the following formula (Nalwa, 2001):

$$\mathrm{LHE} = 1 - 10^{-A} = 1 - 10^{-f} \quad (1)$$

Values of LHE are given in Table 3. LHE values were high (0.706–0.940). From these results we can conclude that comparative to CS1A, Dyes 1–4 with an electron-deficient π-spacer showed better optical properties, which will be fruitful when used in DSSCs.

3.4. Adsorption of dyes on TiO_2 surface

Nature of excited states of semiconductor/dye interface controls the electron injection rate from dye to semiconductor. Hence, the computational modeling of semiconductor/dye interface is a very useful tool to optimize DSSCs. In this regard, simulations of the electronic and optical properties of TiO_2 nanoparticles and the dye excited states were performed.

Semiconductors are one of the main components in the DSSCs and nanostructured TiO_2 has frequently been used in

Table 4 Computed maximum absorption wavelengths (λ_{max}/nm), absorption energy (E_g/eV), oscillator strengths (f), light harvesting efficiency (LHE) and transition natures of dyes@TiO_2 cluster.

Dye	λ_{max}	E_g	f	LHE	Main configurations
CS1A	453	2.88	0.702	0.716	H-2 → L + 11(87%)
1	509	2.40	0.874	0.866	H → L + 8 (77%)
2	539	2.36	1.073	0.915	H-1 → L + 9 (69%)
3	572	2.10	1.191	0.936	H-2 → L + 7 (64%)
4	581	1.96	1.370	0.957	H → L + 6 (55%)

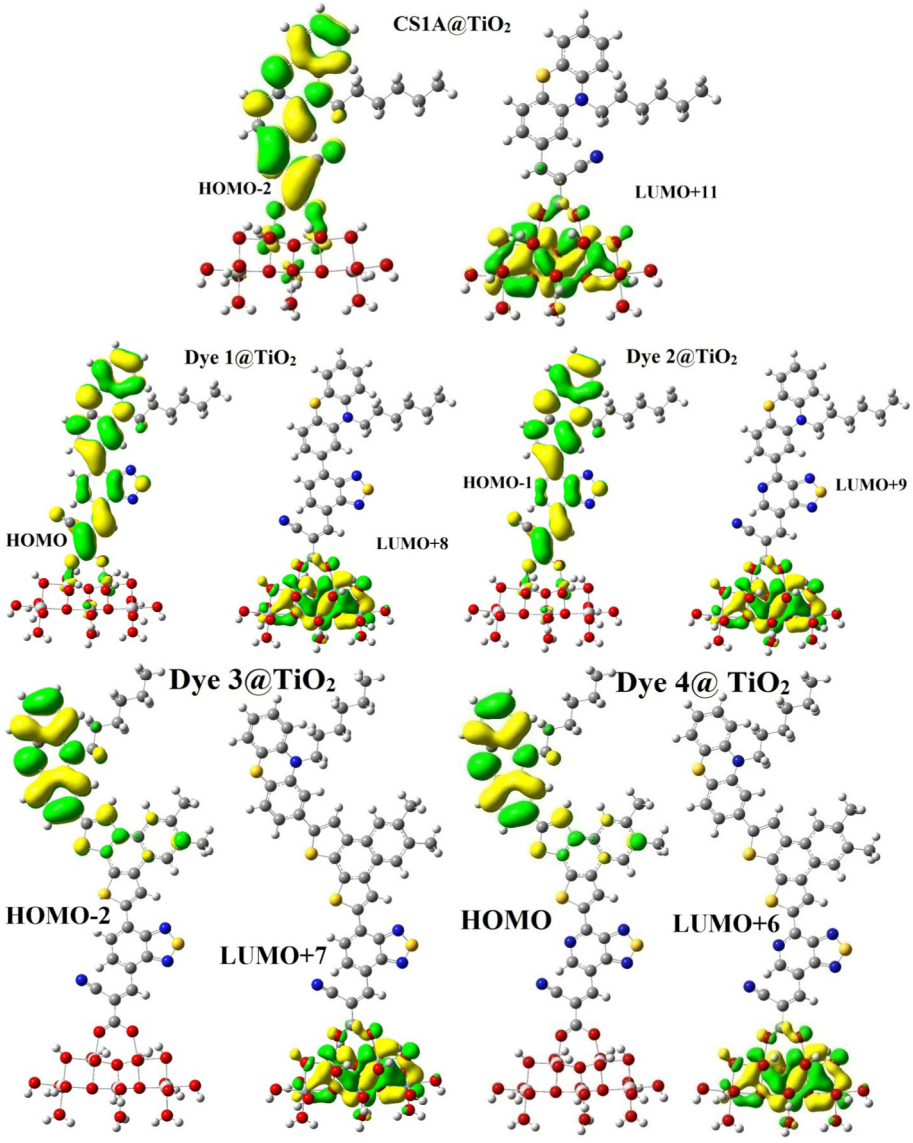

Figure 3 HOMO and LUMO of studied dyes@TiO_2 cluster.

Table 5 ΔG^{inject} (eV), oxidation potential (eV) of dyes.

Dye	ΔG^{inject}	E_{OX}^{dye*}	E_{OX}^{dye}
CS1A	−0.50	2.52	5.50
1	−0.89	3.10	5.60
2	−0.75	3.42	5.82
3	−0.80	3.18	5.33
4	−0.65	3.52	5.52

the most efficient DSSC systems. TiO_2 has three major crystalline structures; rutile, anatase and brookite. However, electrodes in photovoltaic cells are often based on anatase and the (1 0 1) surface of anatase is the thermodynamically most stable surface (Persson et al., 2002). The $Ti_5O_{20}H_{22}$ (1 0 1) model from crystal structures is adopted as the surface of TiO_2 film in the current work. The model is small enough that the large basis set (6–31 + G*) can be adopted in the calculation. From several adsorption configurations, the bidentate chelating adsorption mode is used. It is energetically favorable (Sanchez-de-Armas et al., 2012).

It is found that electronic and optical properties of dyes that showed significant changes when absorbed to TiO_2 might be due to interaction between the dyes and the semiconductor. Therefore, we also simulated the UV/Vis absorption spectra of the dyes after binding to the $Ti_5O_{20}H_{22}$ cluster at the same level of theory for the free dyes except that the LANL2DZ basis set was used for the Ti atom. The results from these investigations are listed in Table 4. We found that after binding to TiO_2, dyes showed red-shift in the maximum absorption wavelengths. Red-shift of the absorption spectra of the dye after binding TiO_2 can be explained on the basis of interactions between the electron acceptor group of the dye (–COOH) and the 3d orbitals of the Ti atom, resulting in an overall decrease in the LUMO energies as compared with the isolated dyes. Oscillating strength (*f*) was improved due to the interaction between

the dyes and the semiconductor compared with the free dyes. HOMOs and LUMOs also demonstrate that there is charge transfer from the donor part to the acceptor $Ti_5O_{20}H_{22}$ (Fig. 3). In addition, after binding to the semiconductor, the LHE of the dyes showed an increase.

3.5. Short-circuit photocurrent density (J_{SC}) and electron injection efficiency

The J_{SC} in DSSCs is determined by the following equation:

$$J_{SC} = \int_{\lambda} \mathrm{LHE}(\lambda)\Phi_{inject.}\eta_{collect.}d\lambda \quad (2)$$

where LHE(λ) is the light harvesting efficiency at a given wavelength, $\Phi_{inject.}$ is the electron injection efficiency, and $\eta_{collect.}$ is the charge collection efficiency. For the same DSSCs with only different dyes, just as for the organic dyes under study, it is reasonable to assume that the $\eta_{collect.}$ is a constant. As a result, the enhancement of J_{SC} should focus on improving the LHE and $\Phi_{inject.}$ According to Eq. (2), in order to obtain a high J_{SC}, the efficient organic dyes used in DSSCs should have a large LHE. The LHE of Dyes 1–4 was higher than that of the CS1A dye.

Another way to enhance J_{SC} is to improve $\Phi_{inject.}$ which is related to the driving force (ΔG^{inject}) of the electron injection from the photoinduced excited states of organic dyes to the TiO_2 surface. In general, a larger ΔG^{inject} leads to a larger Φ_{inject}.

The calculation of the electron injection quantities is important for the interpretation of photovoltaic data. The free energy change (in eV) for the electron injection can be expressed by the following equation, assuming that the electron injection occurs from the unrelaxed excited state:

$$\Delta G^{inject} = E_{OX}^{dye*} - E_{CB}^{TiO_2} \quad (3)$$

where E_{OX}^{dye*} is the oxidation potential of the dye in the excited state, $E_{CB}^{TiO_2}$ is the reduction potential of the conduction band of the TiO_2 $\left(E_{CB}^{TiO_2} = 4.0\,\mathrm{eV}\right)$. It is generally accepted that the electron injection from the photoinduced excited states of organic dyes to the semiconductor occurs before the vibrational relaxation.

$$E_{OX}^{dye*} = E_{OX}^{dye} - \lambda_{\max}^{ICT} \quad (4)$$

where E_{OX}^{dye} is the redox potential of the ground state. E_{OX}^{dye} can be estimated as negative E_{HOMO} (Pearson, 1988), where in this equation $\lambda_{\max}^{ICT}$ is the energy of the intra-molecular charge transfer (ICT). By using this scheme, we calculated ΔG^{inject}, as well as E_{OX}^{dye} and E_{OX}^{dye*} for dyes and the results are listed in Table 4. We found that all the calculated ΔG^{inject} were negative, which means that the dye excited state lies above the TiO_2 conduction band edge, favoring the injection of the electron from the excited state dye to the TiO_2 conduction band edge. From Table 5 it is clear that ΔG^{inject} becomes more negative by adding electron-deficient pi-spacers. Improvement in LHE and driving force (ΔG^{inject}) of the electron injection would show higher J_{SC}. Performance of DSSCs sensitized by Dye 4 might be superior to the other dyes, due to its favorable performances of the above factors based on our computed results. Results of this study also indicate that incorporating electron-deficient pi-spacer is an efficient strategy to improve Short-circuit photocurrent density (J_{SC}).

4. Conclusions

In this study, we have designed phenothiazine based sensitizers using electron-deficient thiadiazole derivatives as the π-spacer. All dyes showed absorbance in the visible region (450–577 nm) with a high oscillator strength (*f*) (0.673–1.223) and light harvesting efficiency (LHE) (0.706–0.940). Compared with the model compound CS1A, the newly designed dyes display significantly enhanced spectral responses in the UV/Vis solar spectrum, due to the significantly much smaller LUMO levels. After binding to titanium oxide, all dyes showed slightly red-shifted absorption (453–581 nm) with an improved oscillator strength (*f*) (0.702–1.370) and light harvesting efficiency (LHE) (0.716–0.957). All dyes showed a high driving force for electron injection, thus leading to a larger J_{SC}. Results of this study show that incorporating electron-deficient thiadiazole derivatives as π-spacer is an efficient strategy to red-shift the absorption maxima of phenothiazine based dyes.

Acknowledgments

The authors would like to sincerely appreciate the Deanship of Scientific Research at King Saud University for funding this research through the Research Group Project no. RGP-VPP-255.

References

Abdullah, M.I., Janjua, M.R.S.A., Nazar, M.F., Mahmood, A., 2013. Quantum chemical designing of efficient TC4-based sensitizers by modification of auxiliary donor and π-spacer. Bull. Chem. Soc. Jpn. 86, 1272–1281.

Agrawal, S., Pastore, M., Marotta, G., Reddy, M.A., Chandrasekharam, M., De Angelis, F., 2013. Optical properties and aggregation of phenothiazine-based dye-sensitizers for solar cells applications: a combined experimental and computational investigation. J. Phys. Chem. C 117, 9613–9622.

Barone, V., Cossi, M., 1998. Quantum calculation of molecular energies and energy gradients in solution by a conductor solvent model. J. Phys. Chem. A 102, 1995–2001.

Boschloo, G., Hagfeldt, A., 2009. Characteristics of the iodide/triiodide redox mediator in dye-sensitized solar cells. Acc. Chem. Res. 42, 1819–1826.

Choi, H., Choi, H., Paek, S., Song, K., Kang, M.-S., Ko, 2010. Novel organic sensitizers with a quinoline unit for efficient dye-sensitized solar cells bull. Korean Chem. Soc. 31, 125–132.

Frisch, M.J., et al., 2009. Gaussian 09, Revision A.1. Gaussian Inc., Wallingford, CT.

Gratzel, M., 2001. Photoelectrochemical cells. Nature 414, 338–344.

Irfan, A., Jin, R., Al-Sehemi, A.G., Asiri, A.M., 2013. Quantum chemical study of the donor-bridge-acceptor triphenylamine based sensitizers. Spectrochim. Acta A 110, 60–66.

Lee, D.H., Lee, M.J., Song, H.M., Song, B.J., Seo, K.D., Pastore, M., Anselmi, C., Fantacci, S., De Angelis, F., Nazeeruddin, M.K., Grätzel, M., Kim, H.K., 2011. Organic dyes incorporating low-band-gap chromophores based on π-extended benzothiadiazole for dye sensitized solar. Dyes Pigm. 91, 192–198.

Lin, J.T., Chen, P.-C., Yen, Y.-S., Hsu, Y.-C., Chou, H.-H., Yeh, M.-C.P., 2009. Organic dyes containing furan moiety for high-performance dye-sensitized solar cells. Org. Lett. 11, 97–100.

Lin, L.Y., Tsai, C.H., Wong, K.T., Huang, T.W., Wu, C.C., Chou, S.H., Lin, F., Chen, S.H., Tsai, A.I., 2011. Efficient organic DSSC sensitizers bearing an electron-deficient pyrimidine as an effective π-spacer. J. Mater. Chem. 21, 5950–5958.

Mishra, A., Fischer, M.K., Bauerle, P., 2009. Metal-free organic dyes for dye-sensitized solar cells: from structure: property relationships to design rules. Angew. Chem. Int. Ed. 48, 2474–2499.

Nalwa, H.S., 2001. Handbook of Advanced Electronic and Photonic Materials and 545 Devices. Academic, San Diego, CA.

Nazeeruddin, M.K., Angelis, F.D., Fantacci, S., Selloni, A., Viscardi, G., Liska, P., Ito, S., Takeru, B., Gratzel, M., 2005. Combined experimental and DFT-TDDFT computational study of photoelectrochemical cell ruthenium sensitizers. J. Am. Chem. Soc. 127, 16835–16847.

O'Regan, B., Grätzel, M., 1991. A low-cost, high-efficiency solar cell based on dye-sensitized colloidal TiO_2 films. Nature 353, 737–740.

Pearson, R.G., 1988. Absolute electronegativity and hardness: application to inorganic chemistry. Inorg. Chem. 27, 734.

Persson, P., Bergström, R., Ojamäe, L., Lunell, S., 2002. Quantum-chemical studies of metal oxides for photoelectrochemical applications. Adv. Quant. Chem. 41, 203–263.

Qin, P., Yang, X.C., Chen, R.K., Sun, L.C., Marinado, T., Edvinsson, T., Boschloo, G., Hagfeldt, A., 2007. Influence of π-conjugation units in organic dyes for dye-sensitized solar cells. J. Phys. Chem. C 111, 1853–1860.

Qiu, X.P., Lu, R., Zhou, H.P., Zhang, X.F., Xu, T.H., Liu, X.L., Zhao, Y.Y., 2008. Synthesis of phenothiazine-functionalized porphyrins with high fluorescent quantum yields. Tetrahedron Lett. 49, 7446–7449.

Sanchez-de-Armas, R., San Miguel, M.A., Oviedo, J., Sanz, J.F., 2012. Coumarin derivatives for dye sensitized solar cells: a TD-DFT study. Phys. Chem. Chem. Phys. 14, 225–233.

Thomas, K.R.J., Baheti, A., Hsu, Y.-C., Ho, K.-C., Lin, J.T., 2011. Electro-optical properties of new anthracene based organic dyes for dye-sensitized solar cells. Dyes Pigm. 91, 33–43.

Tian, H.N., Yang, X.C., Chen, R.K., Zhang, R., Hagfeldt, A., Sun, L.C., 2008. Effect of different dye baths and dye-structures on the performance of dye-sensitized solar cells based on triphenylamine dyes. J. Phys. Chem. C 112, 11023–11033.

Velusamy, M., Thomas, K.R.J., Lin, J.T., Hsu, Y.C., Ho, K.C., 2005. Organic dyes incorporating low-band-gap chromophores for dye-sensitized solar cells. Org. Lett. 7, 1899–1902.

Wong, B.M., Cordaro, J.G., 2008. Coumarin dyes for dye-sensitized solar cells: A long-range-corrected density functional study. J. Chem. Phys. 129, 214703.

Wu, W., Yang, J., Hua, J., Tang, J., Zhang, L., Long, Y., Tian, H., 2010. Efficient and stable dye-sensitized solar cells based on phenothiazine sensitizers with thiophene units. J. Mater. Chem. 20, 1772–1779.

Xu, M.F., Li, R.Z., Pootrakulchote, N., Shi, D., Guo, J., Yi, Z.H., Zakeeruddin, S.M., Grätzel, M., Wang, P., 2008. Energy-level and molecular engineering of organic D-π-A sensitizers in dye-sensitized solar cells. J. Phys. Chem. C 112, 19770–19776.

Yen, Y.-S., Hsu, Y.-C., Lin, J.T., Chang, C.-W., Hsu, C.-P., Yin, D.-J., 2008. Pyrrole-based organic dyes for dye-sensitized solar cells. J. Phys. Chem. C 112, 12557–12567.

Zeng, W.D., Cao, Y.M., Bai, Y., Wang, Y.H., Shi, Y.S., Zhang, M., Wang, F.F., Pan, C.Y., Wang, P., 2010. Efficient dye-sensitized solar cells with an organic photosensitizer featuring orderly conjugated ethylenedioxythiophene and dithienosilole blocks. Chem. Mater. 22, 1915–1925.

Zhang, G.L., Bai, Y., Li, R.Z., Shi, D., Wenger, S., Zakeeruddin, S.M., Gratzel, M., Wang, P., 2009. Employ a bisthienothiophene linker to construct an organic chromophore for efficient and stable dye-sensitized solar cells. Energy Environ. Sci. 2, 92–95.